Role of potential-energy scaling in the low-temperature relaxation behavior of amorphous materials

Frank H. Stillinger
AT&T Bell Laboratories, Murray Hill, New Jersey 07974
(Received 22 March 1985)

Under the assumption that the Kohlrausch-Williams-Watts (KWW) function describes relaxation near the glass transition for amorphous substances, implications are explored for the character of the many-body potential-energy function. The analysis proceeds in several stages: (1) The configuration space is uniquely divided into minimum-containing cells by a steepest-descent construction on the potential hypersurface. (2) Attention is confined to the amorphous region of configuration space by projecting out all cells containing local crystalline patterns. (3) The potential is separated into a hard-core part Φ_c and a "soft" remainder Φ_s. (4) Φ_s is coarse grained (smoothed) over a variable scale of lengths l. (5) A master equation is used to describe the relaxation spectrum subject to the interaction smoothed over any l. The demand that KWW relaxation emerge from the last constrains the statistical topography of Φ_s. Specifically it requires that on widely separated length scales, multiply branched channels of relatively modest elevation change must exist in Φ_s. Furthermore, the separating barriers between these channels tend to be largest in those portions of configuration space sampled by the system at the lowest temperatures, and to scale as $\ln l$.

I. INTRODUCTION

Substances vary widely in the ease with which their liquid states can be supercooled into rigid glasses.[1] On the one hand, it is difficult to prevent pure molten metals from crystallizing, even when they are cooled at the most rapid rates experimentally attainable (10^6 to 10^7 °C/sec). On the other hand, many network-forming substances (B_2O_3, SiO_2, As_2S_3) and hydrogen-bonding organics (glycerol) usually avoid crystallizing even under very slow cooling rates. This distinction hinges at the atomic level on the number and types of particle packings (mechanically stable atomic arrangements) created by the interactions present, and on the frequency with which thermal motion causes them to be interconverted.

The present paper is devoted to a general view of structural relaxation in condensed phases, with emphasis on low-temperature amorphous materials. The descriptive method used is based upon one that has previously been applied to the study of structure and dynamics in dense media, particularly in connection with molecular-dynamics computer simulation.[2-5] Specifically, it identifies the collection of potential-energy minima for the system of interest and then maps arbitrary configurations of the particles onto appropriate members of that collection. This procedure is reviewed in Sec. II. Section III presents the adaptation of the procedure to the supercooled liquid and amorphous glassy states by projecting out all potential minima possessing crystalline order.

Glass-forming substances normally display a remarkable increase in viscosity and in response time to external perturbations as they approach their so-called glass transition temperature T_g. Furthermore, the spectrum of relaxation times in that regime tends to become broad. The Kohlrausch-Williams-Watts (KWW) correlation function[6,7] has provided a convenient and accurate way to express this broad relaxational response (except at very short times) for a wide collection of properties such as density, energy, orientation, elastic properties, and various other measures of atomic-scale order. This correlation function has the following form:[8-11]

$$\xi(t)=\xi_0 \exp[-(t/\tau)^{\beta_0}] . \tag{1.1}$$

Exponent β_0 is found (usually) to lie in the range

$$0.3<\beta_0<1.0 , \tag{1.2}$$

but may vary with substance, and with temperature and pressure for a given substance. The time τ is a strong function of temperature T, and often can be represented by the same type of Tamman-Vogel-Fulcher function that has been used for shear viscosity η:[12]

$$\tau,\eta \cong A \exp[-B/(T-T_0)] , \quad A,B>0, \quad T_g>T_0>0 . \tag{1.3}$$

Several tentative models and rationales for the KWW behavior have been advanced.[13-18] In one respect, the present work differs tactically from those prior studies. Instead of proposing a specific scenario for KWW relaxation to occur, which *might* be applicable to real substances near T_g, it regards KWW relaxation as given and tries to infer what properties consequently *must* be exhibited by the many-body interaction potential Φ. Toward that end we examine statistically the multidimensional topography of Φ over various length scales.

Section IV introduces a spatial coarse-graining operation to smooth out the fine detail present in Φ. This leaves the relevant slow relaxations essentially unchanged and they can be described by a master equation as explained in Sec. V. Section VI employs these concepts to infer the statistical scaling behavior of Φ. Section VII discusses the conclusions and their implications.

II. MAPPING ONTO POTENTIAL MINIMA

Let the material system of interest contain N_1 particles of species 1,2, . . . , N_ν particles of species ν, with

$$N=\sum_{\alpha=1}^{\nu} N_\alpha \ . \tag{2.1}$$

The masses will be denoted by $m_1, m_2, \ldots, m_\nu$. Furthermore, let $\mathbf{r}_{j\alpha}$ represent the position of the jth particle of species α. These positions can all be combined for convenience in a $3N$-dimensional vector $\mathbf{r}$.

Interactions in the system are described by potential-energy function $\Phi(\mathbf{r})$, which can include wall forces if circumstances so require. Φ will be bounded below and at least twice differentiable away from configurations with particle overlap.

Mechanically stable arrangements of the particles ("packings") correspond to local minima of Φ. The absolute minimum presumably arises from the most-nearly-perfect crystalline arrangement of the particles, a single perfect crystal if the stoichiometry is proper, or a mixture of possibly imperfect crystals if it is not. Higher-lying relative minima for Φ will include many different kinds of particle arrangements, specifically those that are homogeneously amorphous.

Aside from cases with vanishing measure, any many-particle configuration can be uniquely referred to or mapped onto a Φ minimum. For this purpose we use a mass-weighted steepest descent on the Φ hypersurface. Starting from the given configuration as an initial condition ($s=0$), the following set of coupled partial-differential equations are then integrated for $s>0$:

$$m_\alpha \frac{\partial \mathbf{r}_{j\alpha}}{\partial s}=-\nabla_{j\alpha}\Phi \ . \tag{2.2}$$

The solution $\mathbf{r}(s)\equiv\{\mathbf{r}_{j\alpha}(s)\}$ moves continuously downward on the Φ hypersurface from the starting point, converging onto a nearby minimum as $s\rightarrow+\infty$. The resulting connections between all possible starting configurations and the minima constitute the desired mapping.

The set of all configurations which map onto the same minimum a defines a cell $\mathbf{C}_a$ surrounding that minimum. The collection of all $\mathbf{C}_a$'s covers the entire configuration space. Two minima a and b whose cells share a boundary face normally will have a saddle point between them which lies in that shared face.

The specific manner in which masses m_α are incorporated into Eqs. (2.2) is motivated by the form of the corresponding Newtonian equations of classical motion:

$$m_\alpha \frac{\partial^2 \mathbf{r}_{j\alpha}}{\partial t^2}=-\nabla_{j\alpha}\Phi \ . \tag{2.3}$$

In particular, that choice means that near Φ extrema the independent solutions to Eqs. (2.2) are given by the harmonic normal modes of Eqs. (2.3) (real frequencies squared in the latter become exponential decay rates in the former). Furthermore, an imaginary-frequency normal mode at a saddle point of Φ in a cell boundary translates precisely into a solution of Eqs. (2.2) that follows the usual "reaction coordinate" across that saddle point.[19]

The mapping just described assumes implicitly that the system volume V is fixed, i.e., that the vessel walls are stationary. Alternatively, it can be assumed that a movable macroscopic piston with area A forms part of the vessel wall, spring loaded to as to impose constant pressure p. It then becomes necessary to append a new configurational coordinate x_0 to the mechanical description, giving the piston position. Potential energy Φ would include x_0 explicitly as a variable, most simply by adding pAx_0 to the interparticle interactions. The set (2.2) of partial differential equations defining the mapping becomes augmented by

$$m_0 \frac{\partial x_0}{\partial s}=-\frac{\partial \Phi}{\partial x_0} \ , \tag{2.4}$$

where m_0 is the piston mass. With this modification the mapping onto discrete minima can proceed essentially as before.

Permutations of identical particles leave Φ unchanged. Hence, each Φ minimum is but one among

$$\Omega_P=\prod_{\alpha=1}^{\nu} N_\alpha ! \tag{2.5}$$

substantially equivalent minima. Aside from this trivial permutational factor the total number Ω of minima will increase exponentially with N in the large-system limit:

$$\Omega\sim\Omega_P \exp(\theta N), \quad \theta>0 \ . \tag{2.6}$$

Justification for the exponential factor rests on the multiplicative character of the number of distinguishable packings: If a system already macroscopic in extent is doubled in size (so V and each N_α double), particle rearrangements in the two halves of the new system can be carried out virtually independently of each other.[2]

In developing the statistical-mechanical theory on the basis of mapping and cellularization in $3N$-dimensional configuration space, it is useful to classify Φ minima by depth. In the large-system limit it is then natural to consider the density of minima along the $\phi=\Phi/N$ axis. The number of distinguishable minima occurring between ϕ and $\phi+d\phi$ can be then written asymptotically:

$$\exp[N\sigma(\phi)]d\phi \ , \tag{2.7}$$

with the assurance that σ is N independent. We have the obvious relation

$$\exp(\theta N)\sim\int \exp[N\sigma(\phi)]d\phi \tag{2.8}$$

and because N is large this implies

$$\theta=\max\sigma(\phi) \ . \tag{2.9}$$

While these general expressions apply equally to constant-volume and to constant-pressure conditions, it must be remembered that σ changes form from one of these alternatives to the other.

Under constant-volume conditions the canonical partition function Q can be exactly expressed as a quadrature over the depth parameter ϕ:[2,3]

$$Q(\beta)=\left[\prod_{\alpha=1}^{\nu}\Lambda_\alpha^{-3N_\alpha}\right]\int \exp\{N[\sigma(\phi)-\beta\phi-\beta f(\beta,\phi)]\}d\phi\ ,$$

$$\beta=(k_BT)^{-1}\ . \quad (2.10)$$

Here, the Λ_α are mean thermal de Broglie wavelengths for the various species and $Nf(\beta,\phi)$ is the mean vibrational free energy for (generally anharmonic) motion in those cells whose minima lie at $\Phi=N\phi$. The Helmholtz free energy and other thermodynamic functions follow from lnQ in the usual fashion.[20]

Constant-pressure conditions generate a partition function Q' with the same superficial form as that shown in Eq. (2.10), except (a) a thermal de Broglie wavelength factor Λ_0^{-1} for the piston degree of freedom must be included, and (b) the functions σ and f must be those appropriate for constant pressure rather than for constant density. The Gibbs free energy subsequently can be extracted from $\ln Q'$.

When N is large, Q (or equivalently Q') can be asymptotically evaluated simply by identifying the maximum of the integrand with respect to ϕ,[2] since the immediate neighborhood of this maximum strongly dominates the integral. The error thereby incurred has no thermodynamic significance. For any given $\beta=(k_BT)^{-1}$ this maximum at $\phi=\phi_m(\beta)$ corresponds to a matching in slopes of σ and of $\beta(\phi+f)$, i.e.,

$$\frac{\partial\sigma}{\partial\phi}=\beta\left[1+\frac{\partial f}{\partial\phi}\right]\ . \quad (2.11)$$

Figure 1 indicates graphically how this last condition is to be satisfied, specifically above the thermodynamic melting temperature. The downward curvature shown by $\beta(\phi+f)$ conforms to the finding that substances become vibrationally "softer" on the average as they become more amorphous.[5,21] Curve segments between A and B, and between A' and B' reflect a dominance in this range of spatially inhomogeneous packings that are partly crystalline, partly amorphous. Subtle shape differences must exist between curves for constant-density and constant-pressure conditions to be consistent with the fact that melting occurs over a nonzero-temperature range only for the former.

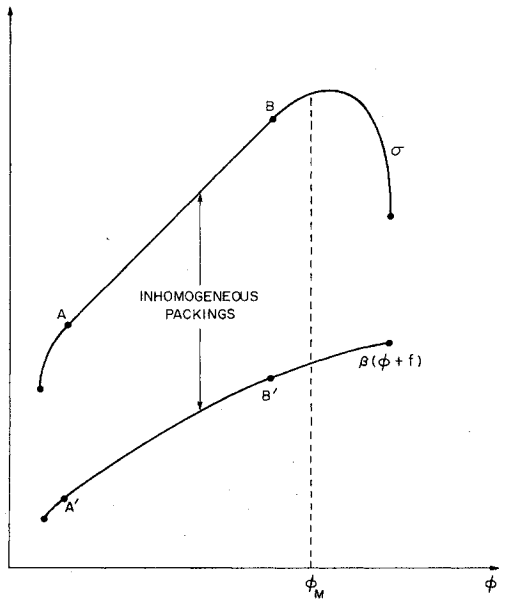

FIG. 1. Graphical construction of $\psi_m(\beta)$ for evaluation of the partition function (Q at constant density, Q' at constant pressure). The case shown corresponds to a temperature above the melting point. Inhomogeneous packings between A and B, and A' and B', contain coexisting crystalline and amorphous regions.

III. SUPERCOOLING AND AMORPHOUS STATES

We now identify a subset of the particle packings which is "crystal free." That is, none of these packings can contain recognizably crystalline arrangements anywhere within their interiors. Projecting this amorphous subset out of the full packing set demands, in principle, a pattern-recognition algorithm. This algorithm is required to identify and to discriminate against occurrence of particle clusters above a minimum size that locally reproduce the crystal pattern within preassigned limits. Precise details are unimportant for present purposes, but a reasonable size limit for discrimination might be a compact set of roughly 20 unit cells, with deformations not to exceed about one-tenth of a lattice spacing.

Materials which successfully avoid crystallization upon cooling below their thermodynamic freezing point remain within that portion of configuration space spanned by cells belonging entirely to the crystal-free or amorphous packing subset. Therefore, it is within this subset that relaxation behavior of the KWW type must find its explanation.

Instead of $\sigma(\phi)$ describing the entire packing distribution by potential energy, the amorphous subset will have a distribution given by $\sigma_1(\phi)$, where obviously

$$\sigma_1(\phi)\leq\sigma(\phi)\ . \quad (3.1)$$

Figure 2 indicates roughly how σ and σ_1 ought to be related. In the high-ϕ regime virtually all packings should be amorphous, so that σ and σ_1 should be nearly (if not exactly) identical. But at point B in Figs. 1 and 2 these functions should begin to separate since σ alone includes cases with coexistent crystalline and amorphous regions. The amorphous-state function σ_1 is a smooth continuation of the common high-ϕ form to ϕ values lower than that at B. However, it must necessarily terminate at a larger minimal ϕ than does σ on account of the noncrystalline constraint involved. It seems reasonable to suppose that both σ and σ_1 equal zero at their respective lower limits as a result of having continuously exhausted available states.

Once the amorphous subset of packings has been isolated by a suitable projection, a mean vibrational free energy $Nf_1(\beta,\phi)$ can be introduced for that subset to replace the former $Nf(\beta,\phi)$. Above point B in Figs. 1 and 2, f_1 should virtually equal f.

To the extent that a supercooled liquid manages to explore the configurations counted by σ_1 in a representative manner, partition functions and free energies can be de-

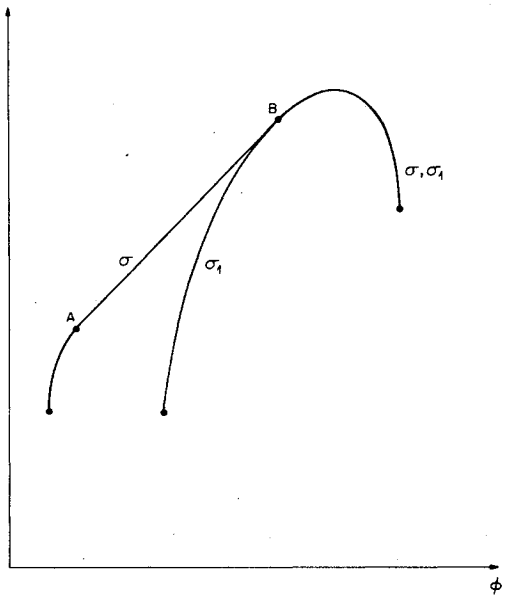

FIG. 2. Schematic relation between σ for the full set of particle packings and σ_1 for the amorphous subset.

fined for that metastable substance. This merely requires replacement of σ and f in Eq. (2.10) (or its constant-pressure analog) by σ_1 and f_1. Once again the ϕ quadrature that results can, for large N, asymptotically be evaluated by picking the integrand maximum. This latter corresponds to a transparent modification of the prior Eq. (2.11), specifically,

$$\frac{\partial\sigma_1}{\partial\phi}=\beta\left[1+\frac{\partial f_1}{\partial\phi}\right] . \tag{3.2}$$

Continued reduction in temperature must eventually foreclose the possibility of a representative sampling of amorphous-packing configuration space, so that Eq. (3.2) and the resulting metastable-state partition function no longer have experimental relevance. This change in behavior is expected to occur near T_g where measurable properties become explicitly dependent on the prior history of the sample under investigation. One of the goals of this work is to clarify the way in which this change arises.

IV. COARSE GRAINING

We now embark on a study of the topography of the Φ hypersurface. It is supposed that the crystal-containing packings have already been projected out of the picture, so subsequent attention focuses strictly on the amorphous-packing portion of configuration space.

The first step involves separating the potential function Φ into two parts:

$$\Phi(\mathbf{r})=\Phi_c(\mathbf{r})+\Phi_s(\mathbf{r}) . \tag{4.1}$$

The first part, Φ_c, represents short-range "core" repulsions that act between any pair of particles at sufficiently small separation. The second part, Φ_s, is the "soft" remainder which includes longer-ranged Coulombic, dipolar, and dispersion interactions.

Although it is not mandatory to do so, ease of exposition warrants treating Φ_c as a set of rigid-core interactions. That is, Φ_c is either infinite or zero according to whether particles geometrically overlap or not. In this circumstance, the set R of configurations without overlap is the physically accessible region of configuration space, and in R we have

$$\Phi(\mathbf{r})\equiv\Phi_s(\mathbf{r}) . \tag{4.2}$$

To the extent that Φ consists of pairwise additive central potentials, the separation would appear as shown in Fig. 3 for each pair. It should be kept in mind that R occupies a fraction of the full amorphous-region configuration space that vanishes exponentially with increasing N; yet, it is in this vanishing portion that low-temperature relaxation behavior is determined.

Previous work[2–5] has demonstrated that the fundamental transitions between cells (passages across saddle points) involve localized particle motions and only change Φ by an amount of order unity. By contrast, the entire span of the depths of minima is of order N. Indeed, laboratory experience with different cooling histories shows that any given glass-forming sample of macroscopic size can be trapped in various Φ minima whose depths also differ by order N. These facts indicate that the Φ hypersurface for glass formers is topographically rough over a wide range of length scales. The objective now is statistical characterization of that scale-dependent roughness.

We next introduce a coarse-graining transformation of Φ_s in R which suppresses small-scale roughness, while preserving the larger-scale features. This coarse graining (smoothing) is accomplished by the following multidimensional integral transform:

$$\Psi(\mathbf{r},l)=\int_R d\mathbf{r}'\,K(\mathbf{r},\mathbf{r}',l)\Phi_s(\mathbf{r}') , \tag{4.3}$$

wherein K is a non-negative kernel defined for $l\geq 0$, which satisfies the conditions

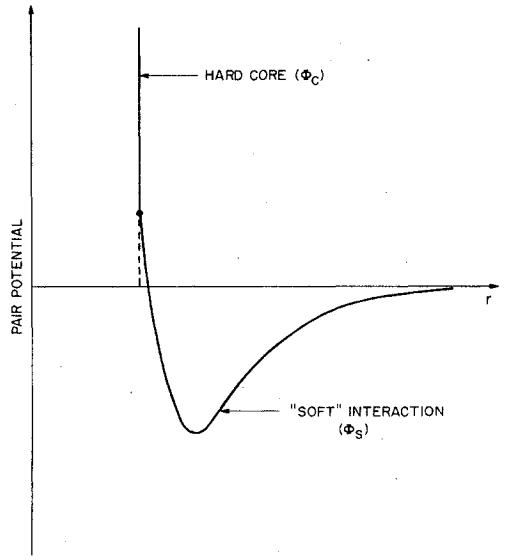

FIG. 3. Typical pair potential showing a hard-core plus longer-range interaction to be consigned, respectively, to Φ_c and to Φ_s, Eq. (4.1).

$$\lim_{l\to 0} K(\mathbf{r},\mathbf{r}',l)=\delta(\mathbf{r}-\mathbf{r}') ,$$
$$\int_R d\mathbf{r}'\, K(\mathbf{r},\mathbf{r}',l)=1 , \tag{4.4}$$
$$(NR)^{-1}\int_R d\mathbf{r}\int_R d\mathbf{r}'\,|\mathbf{r}-\mathbf{r}'|^2 K(\mathbf{r},\mathbf{r}',l)=l^2 .$$

The first of these conditions shows that

$$\Psi(\mathbf{r},0)\equiv\Phi_s(\mathbf{r}) , \tag{4.5}$$

while for positive l, Ψ is a coarse-grained version of Φ_s that involves averaging in each Cartesian direction over, essentially, distance l.

For most of what is to come, K need not be specified further. However, it is useful to keep in mind a concrete realization of this kernel, namely, the solution to the multidimensional diffusion equation in R with vanishing gradient conditions at the hard-core boundary of R:

$$K(\mathbf{r},\mathbf{r}',l(t))=F(\mathbf{r},\mathbf{r}',t),\quad \frac{\partial F}{\partial t}=-D\nabla_{\mathbf{r}}F ,$$
$$\lim_{t\to 0} F=\delta(\mathbf{r}-\mathbf{r}') . \tag{4.6}$$

The "diffusion" clearly causes the root-mean-square distance l to increase monotonically with time at a rate jointly determined by the diffusion constant D and the local geometry of the accessible region R.

As l increases from zero, the coarse-grained potential Ψ becomes ever smoother, eliminating many of the minima originally present in Φ. The number of minima shown in Eq. (2.6) for the unsmoothed potential consequently requires modification to enumerate minima of $\Psi(l)$ in the amorphous region of configuration space:

$$\Omega_1(l)\sim\Omega_P\exp[\theta_1(l)N] , \tag{4.7}$$

where $\theta_1(l)$ decreases monotonically with l. The permutational factor Ω_P remains unchanged, for even after smoothing, any remaining minimum can still be converted into an exactly equivalent one by an interchange of identical particles. Of course, it must be true that Ψ barriers between permutationally equivalent minima become extremely low as l increases.

Just as was the case for the original potential function Φ, configurational mapping to minima can be carried out on the coarse-grained potential Ψ. For this purpose we use the same equations (2.2), but with Ψ replacing Φ in the right-hand members. This mapping on the Ψ hypersurface leads as before to cells $\mathbf{C}_a(l)$ defined as point sets which map to a common minimum a. These cells continue to cover the full configuration space exhaustively and without overlap, but their number decreases strongly with increasing l as Eq. (4.7) indicates, so the mean cell content must increase accordingly:

$$\langle \mathbf{C}_a(l)\rangle \propto \exp[-\theta_1(l)N] . \tag{4.8}$$

The mechanism for cell growth with increasing l involves destabilization of marginally bistable degrees of freedom, as Fig. 4 illustrates. As remarked above, the collective coordinates describing these degrees of freedom involve (at least for small l) motions of small localized groups of particles, and these groups are to be found more

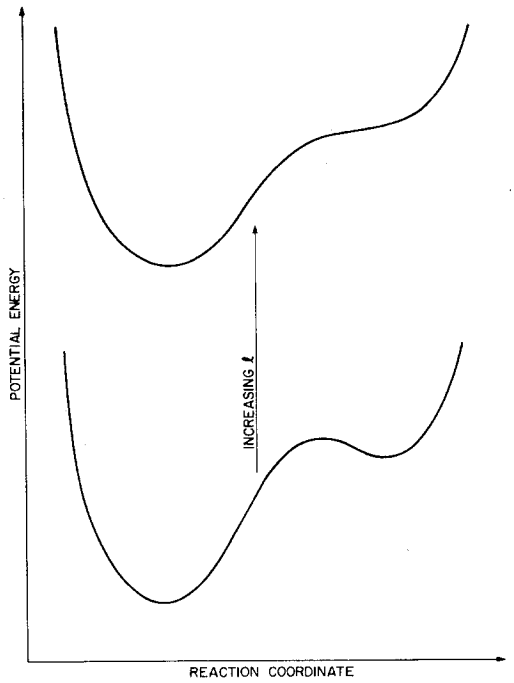

FIG. 4. Basic effect of coarse graining. A marginally bistable degree of freedom is converted to monostability.

or less randomly distributed throughout the entire system. Whenever one of these bistable groups goes monostable, a pair of contiguous cells $\mathbf{C}_a(l)$ and $\mathbf{C}_b(l)$ unite. Actually, the cell with the deeper minimum envelops and consumes its neighbor in an operation of a "survival of the deepest."

The random aggregation of cells to create larger cells will produce dendritic rather than compact objects. So while the number of surviving cells with which a given cell conceivably might unite declines, the boundary along which unification could occur increases in a counterbalancing manner.

It is useful to invert the earlier argument for the multiplicative property that underlies exponential growth with N of the number of distinct minima. We may ask how large a volume $v_M(l)$ would be required on the average so that the number of distinct Ψ packings it contains would be some integer $M>1$. If V is the three-dimensional volume of the system, we must have

$$M^{V/v_M(l)}=\exp[\theta_1(l)N],\quad v_M(l)=V\ln M/[N\theta_1(l)] , \tag{4.9}$$

so that the requisite volume is inversely proportional to $\theta_1(l)$. Formally extending this result down to $M=2$, we obtain an estimate $v_2(l)$ of the size of a locale in the potential-smoothed many-body system, which on the average is still capable of a single binary switch between alternative packings.

Considering that bistable degrees of freedom suffer an attrition as l increases, it is natural to suppose that their concentration declines exponentially with l. Since $v_M(l)$ is inversely proportional to that concentration, we write

$$v_M(l)\sim(V\ln M/N)\exp[h(l)] , \tag{4.10}$$

where simple attrition would require $h(l)$ to increase

linearly with l. We keep open the possibility that the smoothing operation may generate more subtle effects, with

$$h(l)\sim h_\infty l^q , \tag{4.11}$$

where the positive exponent q may differ from unity. From Eq. (4.9) we must have

$$\theta_1(l)=\exp[-h(l)]\sim\exp(-h_\infty l^q) . \tag{4.12}$$

Let ψ denote $\Psi(l)/N$. In extension of the former definition of $\sigma_1(\phi)$, we can introduce the function $\sigma_1(\psi,l)$ to describe the distribution of amorphous-region minima on the Ψ hypersurface. The number of distinguishable minima whose depths (on a per-particle basis) lie between ψ and $\psi+d\psi$ will asymptotically be given by

$$\exp[N\sigma_1(\psi,l)] . \tag{4.13}$$

Furthermore, we have

$$\theta_1(l)=\max_{(\psi)}\sigma_1(\psi,l) , \tag{4.14}$$

in analogy to the earlier Eq. (2.9).

As coarse graining expands and deforms the cells $\mathbf{C}_a(l)$, the cell "vibrational" free energy requires redefinition. We now let $Nf_1(\beta,\psi,l)$ represent the average vibrational free energy for particle motion in the new cells whose minima lie at $\Psi\equiv N\psi$. Evidently, f_1 should monotonically decrease as l increases, as a result of average cell growth.

Partition functions [such as that in Eq. (2.10)] and their free energies are not invariant under coarse graining. However, the analog to Eq. (3.2),

$$\frac{\partial\sigma_1(\psi,l)}{\partial\psi}=\beta\left[1+\frac{\partial f_1(\beta,\psi,l)}{\partial\psi}\right] , \tag{4.15}$$

can still be invoked to identify $\psi_m(\beta,l)$, the dominant depth for visited minima on the $\Psi(l)$ hypersurface when temperature is given by $\beta=(k_BT)^{-1}$. Of course, this presumes that the amorphous-packing portions of the hypersurface can still be sampled kinetically in a representative fashion, if not with full ergodicity,

V. MASTER EQUATION

We have remarked above that even after coarse graining, potential minima and their cells continue to occur in equivalence classes that each contain Ω_P members. Virtually all physical properties whose relaxations are of interest correspond to dynamical variables that are symmetric under permutation of identical particles. Therefore, measurable relaxation is connected with probability flow in configuration space between different equivalence classes of cells. In order to describe that relaxation we shall use a master equation for time-dependent residence probabilities in those equivalence classes.

When the coarse-graining procedure has been carried out over distance l, the number of equivalence classes (i.e., the number of distinct ways of packing the particles) in the amorphous part of configuration space is

$$Y(l)\equiv\exp[\theta_1(l)N] . \tag{5.1}$$

Let $P_i(t)$ stand for the probability at time t that the system lies in the union of Ω_P cells for the ith equivalence class. By definition we must have the conservation condition

$$\sum_{i=1}^{Y}P_i(t)=1 . \tag{5.2}$$

The master equation describing time dependence of the P_i's has the following form:[22]

$$\frac{dP_i}{dt}=\sum_{j\,(\neq i)}[L_{ji}(E)P_j(t)-L_{ij}(E)P_i(t)] . \tag{5.3}$$

Here, it is assumed that the dynamical system has a conserved total energy E, and the transition probability at this fixed energy from equivalence class j to equivalence class i has been denoted by $L_{ji}(E)$. The reverse rate has been denoted by $L_{ij}(E)$. The time-independent equilibrium state is characterized by probabilities

$$P_i^{(0)}=M_i(E)\Big/\sum_j M_j(E)\geq 0 , \tag{5.4}$$

where $M_i(E)$ is the total phase-space measure for those cells comprising "i."

Detailed balance requires that the transition rates have the form

$$L_{ij}(E)=B_{ij}(E)/M_i(E) , \tag{5.5}$$

where B_{ij} is a symmetric transmission coefficient:

$$B_{ij}(E)=B_{ji}(E) . \tag{5.6}$$

Barring accidental degeneracy, the general solution to the master equation can be expressed as a linear combination of decaying exponentials:

$$P_i(t)=\sum_n A_n\chi_i^{(n)}\exp(-\lambda_n t) . \tag{5.7}$$

Here, the $\chi_i^{(n)}$ and λ_n are eigenvector components and eigenvalues for the $Y\times Y$ operator L:

$$L\cdot\chi^{(n)}=\lambda_n\chi^{(n)} , \tag{5.8}$$

where L has elements

$$\begin{aligned}(L)_{ij}&=-L_{ji}(E)\quad(i\neq j) ,\\ (L)_{ii}&=\sum_{j\,(\neq i)}L_{ij}(E) .\end{aligned} \tag{5.9}$$

We suppose that the $\chi^{(n)}$ are orthonormal:

$$\chi^{(m)}\cdot\chi^{(n)}=\delta_{mn} . \tag{5.10}$$

Thermal equilibrium at energy E corresponds to the single vanishing eigenvalue $\lambda_0=0$; all other eigenvalues are positive.

By increasing l, the number $Y(l)$ of eigenvectors and eigenvalues will decrease in accordance with Eqs. (4.12) and (5.1). The resulting thinning out of the spectrum of L mostly affects the large λ_n's. The equilibrium-state eigenvalue $\lambda_0=0$, of course, persists for all l. Those λ_n that are small and positive should remain virtually unchanged until l becomes very large because they describe

slow reequilibration processes over large-scale topographic features that are themselves unaffected by operations that smooth out only small-scale features.

Let F be a property whose average value at "equilibrium" for the given energy E vanishes. A case in point might set F equal to the z component of the dipole moment for a single test molecule placed in the amorphous medium, so relaxation of initial orientation to isotropy ($F=0$) measures the rate of local kinetic processes. Suppose that F can be assigned mean values F_i appropriate for the interiors of each of the cell equivalence classes. Then the time dependence of the regression of an initial fluctuation in F is simply to be written

$$\bar{F}(t)=\sum_i F_i P_i(t) . \tag{5.11}$$

By inserting Eq. (5.7) this becomes

$$\bar{F}(t)=\sum_n A_n \left[\sum_i \chi_i^{(n)} F_i \right] \exp(-\lambda_n t) . \tag{5.12}$$

Because $\chi_i^{(0)}$ is proportional to the equilibrium populations $P_i^{(0)}$, the F_i must obey

$$\sum_i \chi_i^{(0)} F_i = 0 , \tag{5.13}$$

so that indeed expression (5.12) decays to zero. In fact, for the majority of eigenvectors (particularly those with relatively large λ_n), we expect to have

$$\sum_i \chi_i^{(n)} F_i \cong 0 , \tag{5.14}$$

since these $\chi_i^{(n)}$ will frequently alternate in sign over those cell classes for which F_i is substantially constant. This is connected intimately with the fact that fundamental transitions are highly localized in space, and only those which occur near the test particle measured by F will contribute to relaxation. Put another way, only those eigenfunctions $\chi^{(n)}$ will contribute to Eq. (5.12), whose sign changes occur solely in association with fundamental transitions near the test particle. This principle of local influence is just what common physical intuition would demand.

VI. IMPLICATIONS OF EXPERIMENT

We are finally in a position to draw inferences from the experimental requirement that the general regression expression (5.12) have the KWW form (1.1) near the glass transition. First, we write $\xi(t)$ in Eq. (1.1) as a Laplace transform:

$$\xi(t)=\xi_0 \int_0^\infty Z(\lambda)\exp(-\lambda t)d\lambda , \tag{6.1}$$

so that $Z(\lambda)$ formally plays the role of a spectral density of measurable relaxation rates. It can be shown[23] that Z has the following behavior for small positive λ:

$$Z(\lambda)=Z_0 \exp[-A(\tau\lambda)^{-p}+o(\lambda^{-p})] , \tag{6.2}$$

where $Z_0>0$ and

$$p=\beta_0/(1-\beta_0), \quad A=(1-\beta_0)\beta_0^{\beta_0/(1-\beta_0)} . \tag{6.3}$$

Consequently, the spectral density vanishes strongly as $\lambda\to 0+$, and it is the precise manner in which that vanishing occurs, which controls the characteristic long time behavior of the KWW function.

The cumulative spectral density for $Z(\lambda)$ has a small-λ form that is also generically the same as that shown in Eq. (6.2):

$$\int_0^\lambda Z(\lambda')d\lambda' = Z_1 \exp[-A(\tau\lambda)^{-p}+o(\lambda^{-p})], \quad Z_1>0 . \tag{6.4}$$

The advantage of the coarse-graining procedure is that it allows this cumulative spectral density at given λ to be identified with the local density of available configurational switches for an appropriate l choice. As l increases, the relatively few remaining effective modes of relaxation are slow, are associated with localized repackings of particles near the test particle, and are substantially equal in number to the cumulative spectral density up to the effective upper limit on λ. Consequently, after having used Eq. (4.10) to fix the density of "switches," we have, to the requisite order,

$$\exp[-h(l)]\cong\exp[-(\tau\lambda)^{-p}], \quad \tau\lambda\cong[h(l)]^{-l/p} . \tag{6.5}$$

It should be stressed that this expression relates l to the effective upper λ cutoff for those surviving terms in regression formula (5.12) when the potential has been smoothed over that distance l.

By appeal to the conventional wisdom of transition-state theory,[24] the rate λ in Eq. (6.5) will be determined by a mean free-energy barrier height $b(l)$ between contiguous cells that must be surmounted on the $\Psi(l)$ hypersurface for relaxation to occur. That is,

$$\lambda\cong(\tau_0)^{-1}\exp[-\beta b(l)], \quad \beta=(k_B T)^{-1} , \tag{6.6}$$

where the pre-exponential factor is an appropriate attempt frequency (assumed to be l independent, consistent with the dendritic character of the cells). Combining Eqs. (6.5) and (6.6), we find

$$b(l)\simeq\beta^{-1}\ln(\tau/\tau_0)+[(1-\beta_0)/\beta_0\beta]\ln h(l) , \tag{6.7}$$

where p has been eliminated in favor of the KWW exponent β_0.

The mean barrier height $b(l)$ contains both potential-energy and entropy components. For any reasonable behavior of the $\Psi(l)$ hypersurface the former component dominates (or at least is not dominated by) the latter. Consequently, we can take Eq. (6.7) to be a statement about the mean height of potential-energy barriers $\Delta\Psi$. Substituting from Eq. (4.11),

$$\Delta\Psi(l)\cong\beta^{-1}\ln(\tau/\tau_0)+[(1-\beta_0)/\beta_0\beta]\ln(h_\infty l^q) . \tag{6.8}$$

This is our principal result. It indicates that barrier heights for kinetically important transitions only rise logarithmically with length scale l. The currently uncertain exponent q only appears as a multiplier for that logarithmic term.

VII. DISCUSSION

It was stressed earlier in connection with Eqs. (2.11), (3.2), and (4.15) that change in temperature causes dif-

ferent portions of the Φ or Ψ hypersurfaces [corresponding to $\phi_m(\beta)$ or $\psi_m(\beta,l)$, respectively] to be preferentially explored. One generally must expect topographic features to be variable from one of these portions to another. This property is clearly manifest in result (6.8) by the explicit appearance of β and even more importantly by the appearance of the time τ. If the Tamman-Vogel-Fulcher equation (1.3) accurately represents the temperature dependence of τ near the glass transition, it is clear from Eq. (6.8) that at fixed l, barrier heights increase strongly with declining temperature. This is an entirely reasonable conclusion: The deeper potential minima probed at lower temperatures are fewer in number and further apart, so that passage from one to another on the average requires ascent over a larger intervening topographic feature. The glass transition temperature T_g represents the stage at which dynamics on the experimentally available time scale is no longer able to provide equilibrating transitions between these increasingly isolated regions of configuration space.

Equation (6.8) also presents a more subtle aspect of temperature dependence, namely the l dependence of mean barrier height, established to be proportional to $\ln l$, must also be expected to vary in strength from high- to low-temperature regions of the Ψ hypersurface. We have seen that the multiplier of $\ln l$ in Eq. (6.8) involves the KWW exponent β_0 and so the statistical topography appropriate for the region explored at a given temperature thus determines β_0. This logical connection helps to interpret the temperature dependence that has occasionally been reported[9] for β_0.

Exponential size growth with l of the cells on the $\Psi(l)$ hypersurface, coupled with mere logarithmic growth with l of kinetically significant intervening barriers, leads to an interesting picture of the relevant topography, namely, over a wide range of length scales, multiply branched channels with relatively modest internal elevation change must exist in the physically accessible region R. This picture can probably be argued as being consistent with at least some of the published models[17,18,25] for relaxation near T_g; however, it is apparently more general and may aid in the construction of new models.

Finally, it is worth emphasizing that computer-simulation studies of glass-forming substances are capable of adding quantitative detail to the qualitative analysis that has been developed here. Contiguous pairs of potential minima, the intervening transition states, and the corresponding reaction coordinates connecting them can and have been studied[26] in isolation. What is now required is a more global view of the way in which these pairs of minima are arranged relative to one another to create the full multidimensional transition network.

[1]J. M. Stevels, in *Handbuch der Physik,* edited by S. Flügge (Springer, Berlin, 1962), Vol. XIII, pp. 510—645.

[2]F. H. Stillinger and T. A. Weber, Phys. Rev. A **25**, 978 (1982).

[3]F. H. Stillinger and T. A. Weber, J. Phys. Chem. **87**, 2833 (1983).

[4]F. H. Stillinger and T. A. Weber, Phys. Rev. A **28**, 2408 (1983).

[5]F. H. Stillinger and T. A. Weber, Science **225**, 983 (1984).

[6]R. Kohlrausch, Ann. Phys. (Leipzig), **12**, 393 (1847).

[7]G. Williams and D. C. Watts, Trans. Faraday Soc. **66**, 80 (1970).

[8]H. S. Chen and M. Goldstein, J. Appl. Phys. 43, 1642 (1972).

[9]J. A. Bucaro, H. D. Dardy, and R. D. Corsaro, J. Appl. Phys. **46**, 741 (1975).

[10]C. C. Lai, P. B. Macedo, and C. J. Montrose, J. Am. Ceram. Soc. **58**, 120 (1975).

[11]G. D. Patterson, C. P. Lindsey, and J. R. Stevens, J. Chem. Phys. **70**, 643 (1979).

[12]A. R. Ubbelohde, *The Molten State of Matter* (Wiley, New York, 1978), p. 414.

[13]A. M. Jamieson, R. Simha, H. Lee, and J. Tribone, Ann. N.Y. Acad. Sci **371**, 186 (1981); see also subsequent comment by S. F. Edwards, p. 197.

[14]M. H. Cohen and G. S. Grest, Ann. N.Y. Acad. Sci. **371**, 199 (1981).

[15]K. L. Ngai, Comments Solid State Phys. **9**, 127 (1979); **9**, 141 (1980).

[16]M. F. Schlesinger and E. W. Montroll, Proc. Nat. Acad. Sci. U.S.A. **81**, 1280 (1984).

[17]R. G. Palmer, D. L. Stein, E. Abrahams, and P. W. Anderson, Phys. Rev. Lett. **53**, 958 (1984).

[18]S. A. Brawer, J. Chem. Phys. **81**, 954 (1984).

[19]K. Ishida, K. Morokuma, and A. Komornicki, J. Chem. Phys. **66**, 2153 (1966).

[20]J. E. Mayer and M. G. Mayer, *Statistical Mechanics* (Wiley, New York, 1940), p. 235.

[21]F. H. Stillinger and T. A. Weber, J. Chem. Phys. **81**, 5095 (1984).

[22]C. Kittel, *Elementary Statistical Physics* (Wiley, New York, 1958), p. 169.

[23]E. Helfand, J. Chem. Phys. **78**, 1931 (1983).

[24]K. J. Laidler and M. C. King, J. Phys. Chem. **87**, 2657 (1983).

[25]G. H. Fredrickson and H. C. Andersen, Phys. Rev. Lett. **53**, 1244 (1984).

[26]T. A. Weber and F. H. Stillinger, Phys. Rev. B **31**, 1954 (1985).